ELSEVIER

Chemical Engineering Journal 72 (1999) 235–244

Chemical Engineering Journal

Characterizing gas and solids distributors with heat transfer study in a gas–solids downer reactor

Y. Ma, J.-X. Zhu*

Department of Chemical and Biochemical Engineering, University of Western Ontario, London, Ont. N6A 5B9, Canada

Received 25 May 1998; received in revised form 16 November 1998; accepted 28 November 1998

Abstract

The heat transfer behavior between the gas–solids flow suspension and a small suspended surface near the distributor region was employed to study the characteristics of the gas and solids distributors with five different distributor designs in a gas–solids co-current downflow fluidized bed (downer) of 9.3 m high and 100 mm i.d., using FCC particles. The radial distributions of heat transfer coefficient between the small suspended surface and the gas–solids flow suspension at several axial levels in the entrance region were obtained using a miniature cylindrical heat transfer probe, with different types of distributors and at various operating conditions. It is shown that the effects of the distributor design on the gas–solids flow can be characterized using the heat transfer techniques, given the close relationship between heat transfer and solids concentration. Furthermore, the radial distributions of the heat transfer coefficient have distinct variations under different types of distributors. The heat transfer results indicate that the distributor structure can significantly affect the gas and solids flow pattern and flow development in the entrance section of the downer.

Keywords: Downer; Distributor; Heat transfer; Solids concentration; Flow development

1. Introduction

Circulating fluidized bed reactors are efficient gas–solid reactors and thus have been widely accepted for various commercial processes [1]. Compared with conventional bubbling bed reactors, the circulating upflow fluidized beds have such advantages as high gas–solids contact and reduced axial dispersion of both gas and solids, but they still suffer from nonuniform radial gas and solids flow. A cocurrent downflow circulating fluidized bed (downer) is a new alternative type of chemical reactor which can overcome this shortcoming. In the downer, because both the gas and solids flow downwards, in the same direction as gravity, the radial gas and solids flow structures are much more uniform than those in the riser [2–5]. This leads to the uniform distribution of particles and more uniform contact time between the gas and solids. Due to these significant advantages, downer reactors have been proposed for some processes such as fluid catalytic cracking (FCC), where short contact time and uniform gas and solids residence time distribution are extremely important. Because the gas and solids residence time is usually very short in the downer, the initial gas and solids flow development is very important in order to control the reaction selectivity and product distribution. However, the majority of the previous research in the downer concentrated in the fully developed section [3,5,6]. In order to optimize the downer for industrial applications, the mechanisms for flow development and acceleration in the entrance section must be investigated. Apparently, the downer distributor design would have an important effect on the gas–solids flow structure in the downer, especially in the entrance section. A good distributor would provide excellent gas–solids mixing and uniform distributions of gas and solids over the column cross-section in order to enhance the flow development. For this reason, it is important to study the effects of various distributor designs on the gas and solids flow distribution in the downer reactor.

Usually, such studies are carried out by directly measuring the solids concentration and particle velocity [7,8], a rather tedious experimental process which requires much time to collect and process the data. In this study, a thermal method was used to characterize the downer distributors. Heat transfer behaviors in circulating fluidized beds have been shown to be directly related to the gas–solids flow conditions [9,10]. Employing this characteristics, this study focuses on the effect of distributor on the heat transfer which is dependent on the gas and solids flow structures in the entrance

*Corresponding author. Fax: +1-519-661-3498; e-mail: jzhu@julian.uwo.ca

1385-8947/99/$ – see front matter
PII: S1385-8947(99)00009-1

section of the downer. The radial distributions of the heat transfer coefficient were measured with five different types of distributors under various operating conditions. These results can reflect the effect of distributors on the gas and solids flow structure in the same section. Because the measurement method for heat transfer is relatively easier than those for measuring the solids concentration and velocity, it provides a simpler tool to achieve the understanding of the effect of distributor design on the hydrodynamics in the downer reactor. In addition, employing heat transfer results to characterize the different distributor designs provides another benefit: the gas–solids mixing effect is also included given the similarities between mass and heat transfer.

2. Experimental equipment and procedure

The experiment was conducted in a riser/downer circulating fluidized bed made of Plexiglas, with a downer of 100 mm in inner diameter and 9.3 m in height as shown in Fig. 1. Solids are entrained upwards in the accompanying riser of diameter 100 mm and height 15.1 m, to the top of the riser where the gas is separated and the solids are fed into the downer through a solids distributor. Separate air sources were used for the riser and downer. At the bottom of the downer, the gas–solids suspension enters the fast separator where most of the entrained solids are recovered. The remaining solids are then separated by two additional cyclones. The solids circulation rate is regulated using a

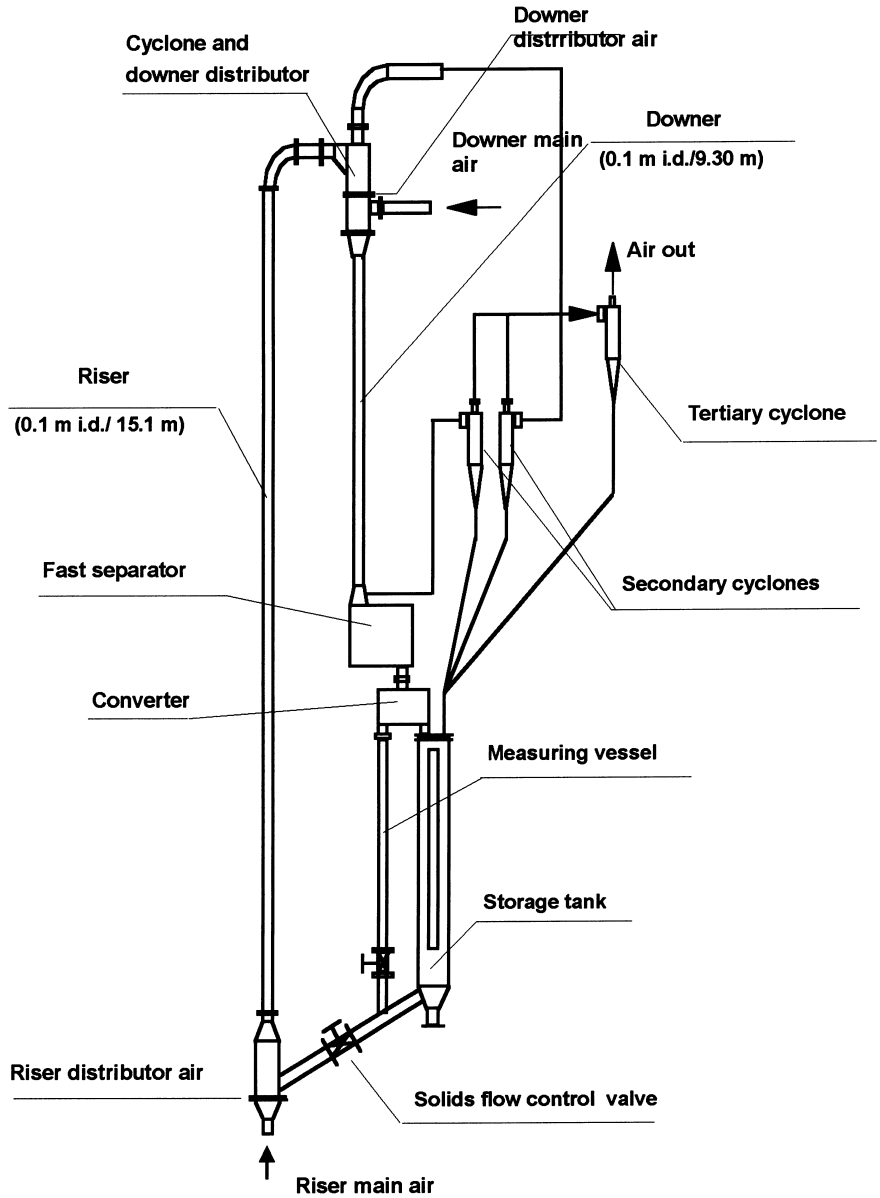

Fig. 1. Schematic of the riser/downer circulating fluidized bed.

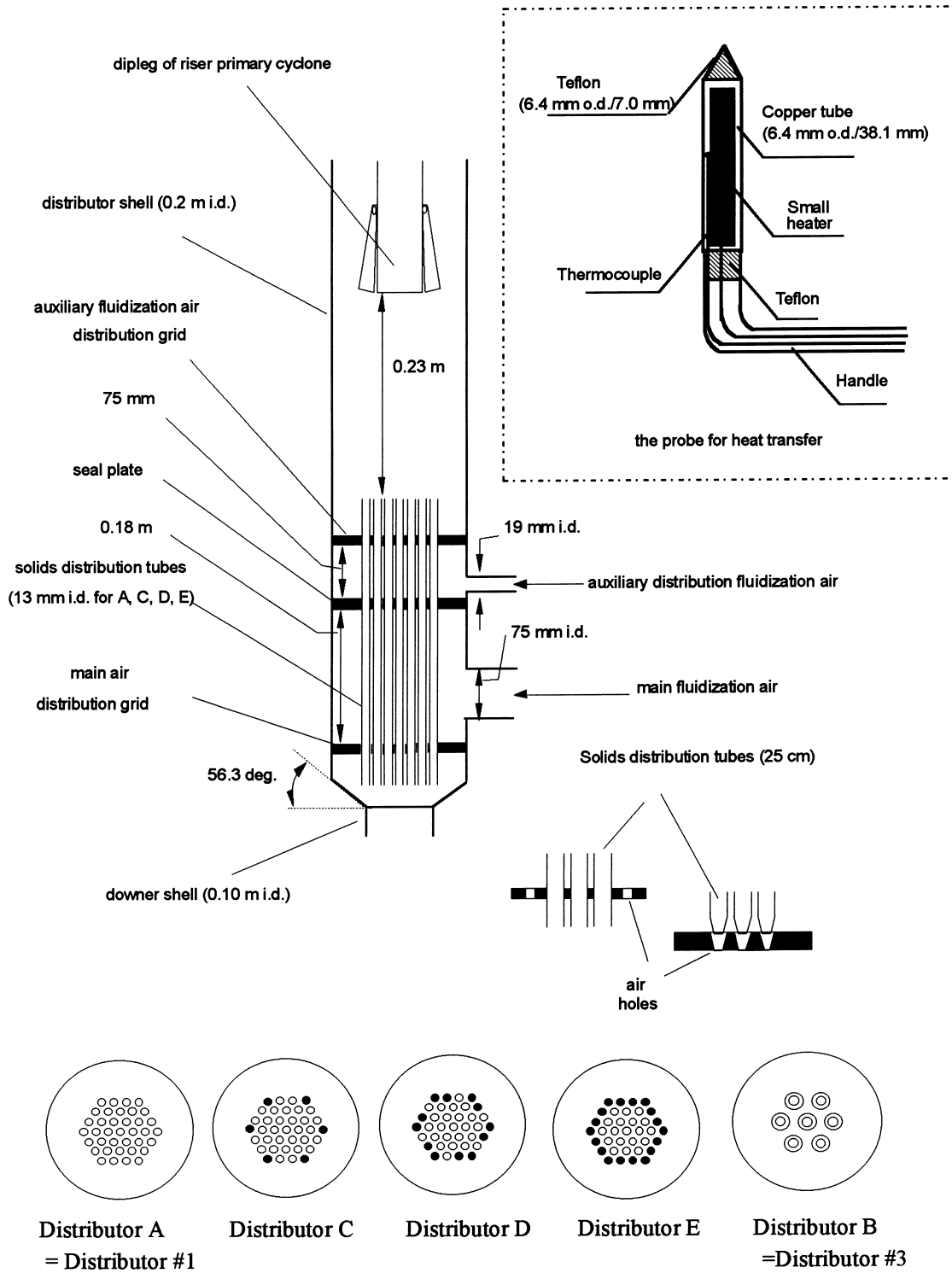

Fig. 2. Schematic of the distributor design and the probe for heat transfer.

solids control valve and can be measured by deflecting the collected solids into the measuring tank (Fig. 1).

Fig. 2 provides the five different distributor designs used in this study. For these designs, solids from the dipleg of the riser primary cyclone are kept under minimum fluidization above the top distributor plate in the downer feed section and are then fed into the downer through the solids distribution tubes. Distributor A (DA) was comprised of 37 vertical distribution tubes of diameter 12.7 mm with an equilateral pitch length of 19.1 mm. Gas is distributed through a 9.53 mm thick plate with 37 holes of 16.7 mm i.d. which encircle the 37 solids distribution tubes. This

Table 1
Operating conditions in this study

Distributor A		Distributor B			Distributor C		Distributor D		Distributor E	
U_g (m/s)	G_s (kg/m^{2}s)	U_g (m/s)	G_s (kg/m^{2}s)	V_n (m/s)	U_g (m/s)	G_s (kg/m^{2}s)	U_g (m/s)	G_s (kg/m^{2}s)	U_g (m/s)	G_s (kg/m^{2}s)
7.6	50	7.6	50	75	7.6	81	7.6	63	7.6	70
7.6	98	7.6	98	75	7.6	140	7.6	140	7.6	130
7.6	150	7.6	150	75						
7.6	180	7.6	180	75						
5.2	98	5.2	98	110						
9.3	98	9.3	98	95						

plate is at a distance of 50.8 mm above the exit of the solids feed tubes, so that gas is distributed upstream, through the 2 mm gaps, before solids enter the downer. This distributor is designed to provide uniform distributions of solids and gas over the downer cross-section. Distributor B (DB) has seven solids distribution tubes of 25.4 mm i.d. with a pitch length of 34.9 mm. To enhance gas–solids mixing, seven brass fittings, characterized with a 12.7 mm length and an internal angle of 70°, are pushed onto the bottom of the solids feed tubes to provide a nozzle effect. The gas distributor, located at the bottom ends of the solids distributor tubes, is characterized by seven nozzles with the same geometry (12.7 mm length and 70° internal angle) as the brass conical fittings on each solids feed tube. Air is distributed through the adjustable gaps formed by the brass nozzles and the 12.7 mm thick acrylic distribution plate. From the nozzle open area, downer cross-sectional area and superficial gas velocity, the nozzle velocity, V_n, can be estimated. The operating conditions are provided in Table 1. With this arrangement, the gas impinges from all directions upon the solids stream from each of the solids feed tubes. Distributors C, D and E (DC, DD, DE) are modifications of DA. To investigate the effects of solids distribution on the initial radial solids distribution, six solids distribution tubes at the corner are plugged for DC, 12 solids distribution tubes are plugged for DD, and 18 solids distribution tubes at the periphery are all plugged for DE.

The particulate solids used for this study were fluid cracking catalyst, FCC. The particles have a wide size distribution with a mean diameter of 67 μm, a particle density of 1500 kg/m^3, and a bulk particle density of 850 kg/m^3.

A miniature cylindrical heat transfer probe (6.4 mm o.d. and 38 mm in length) was inserted into the column to measure the local heat transfer coefficients. As shown in Fig. 2, the probe is made of a 6.4 mm diameter and 1.5 mm wall thickness copper tube with a small cartridge heater (50 Watts) enclosed inside and thermally insulated by Teflon at both ends. A thermocouple is enclosed into the copper wall to read the surface temperature. During the measurements, the probe was positioned upwards to minimize its influence on the flow, and the probe was traversed along the radial direction. Considering the high gas and solids flow, the vigorous mixing and the small amount of heat generated by the probe, the temperature of the gas–solids suspension can be considered constant and uniform. With this assumption and the assumption of minimal heat losses through the Teflon ends, the following equation can be used to calculate the local heat transfer coefficient:

$$h = \frac{IV}{A(T_s - T_b)}, \quad (1)$$

where T_s is the probe surface temperature (30°C<T_s<40°C) and T_b is the average bed temperature (20°C<T_b<30°C), measured by a thermocouple inserted inside the bed down stream of the probe.

For this study, heat transfer coefficients were measured at 10 radial positions on different longitudinal heights (0.2, 0.9, 1.6, 4.5, 6.0 m from the solids distribution tube ends) below the downer distributor. The superficial gas velocity was ranged from 5.2 to 9.6 m/s, and the solids circulation rate from 46 to 180 kg/m^{2}s (Table 1). For comparison, some additional experiments were also performed using an optical fiber probe to measure the local solids concentration. Details of the fiber optic probe are given elsewhere [11].

3. Experimental results and discussion

3.1. The relationship between heat transfer and solids concentration

The solids concentration is the dominant operating parameter influencing the heat transfer in a circulating fluidized bed [9,10]. Wu et al. [9] found that the local instantaneous heat transfer coefficient between the gas–solids suspension and a suspended surface is directly related to the local solids concentration as shown in Fig. 3(a). Lockhart et al. [10] measured the local solids concentration distribution and local heat transfer coefficients around the membrane wall in a riser reactor and clearly showed that higher heat transfer at the fin corresponds to higher solids concentration (Fig. 3(b)). They showed that there is a fixed linear relationship between the local time-average heat transfer coefficients and the local time-average solids concentrations. The same situation was found in this study: the heat transfer coefficient and the solids concentration under similar operating conditions were well correlated with different types of

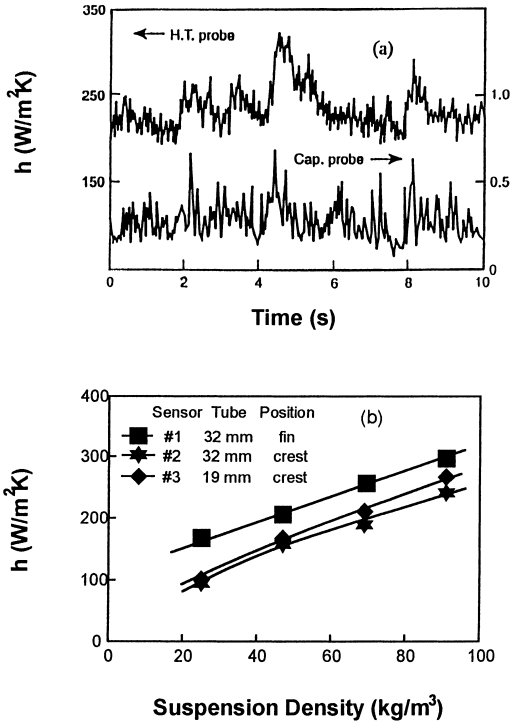

Fig. 3. The relationship between heat transfer coefficient and local solids concentration (a) Wu et al. [15]; (b) Lockhart et al. [10]

distributors. Fig. 4 shows radial distributions of heat transfer coefficient and solids holdup with DA and DB. It can be found that the distribution profiles of the heat transfer coefficient are very consistent with those of the solids holdup, even though the different structures of the distributors lead to different gas and solids flow structures and significantly alter the initial solids holdup and heat transfer coefficient distributions below the distributors. Under distributor A, both the heat transfer coefficient and the solid holdup remain nearly uniform in the central region, then increase to form a peak at the same radial position $r/R = 0.85 \sim 0.90$, and finally drop towards the wall. With distributor B, due to the high velocity gas jet, the heat transfer coefficient and solids holdup are both more uniform in the radial direction, except for a slight increase approaching the wall. These results confirm that the close relationship between heat transfer and solids concentration also exists in the downer. Therefore, the results for the radial distributions of heat transfer coefficients with different types of distributors can reflect the effects of the distributors on the distributions of solids concentration and the gas and solid flow development immediately below the distributors.

3.2. Radial distributions of heat transfer coefficient with distributors A and B

Fig. 5 shows the radial distributions of heat transfer coefficient at different axial positions measured with

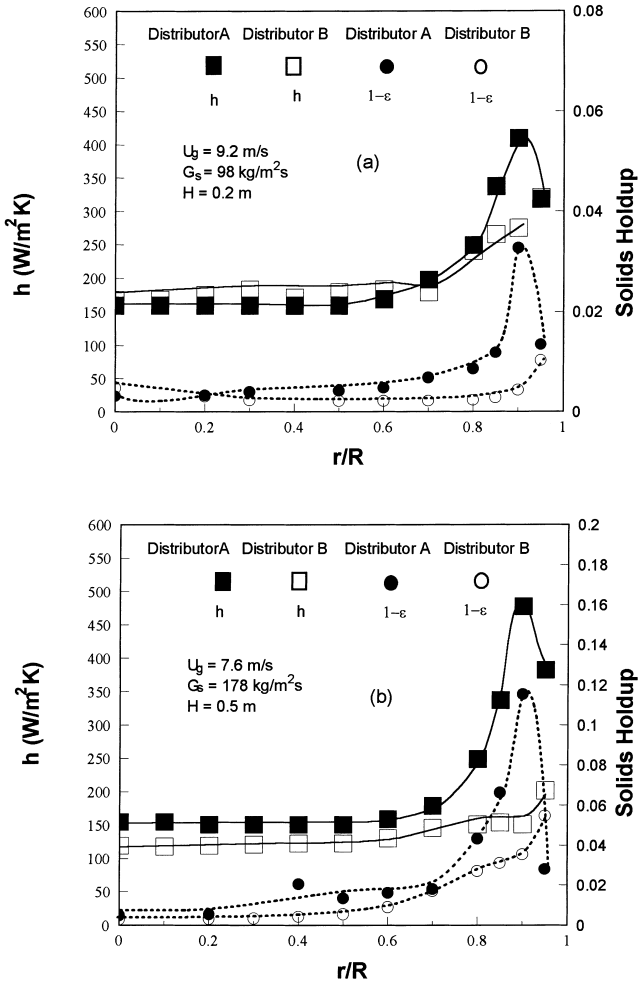

Fig. 4. The relationship between the heat transfer coefficient and the local solids concentration with distributors A and B.

distributor A. Near the distributor ($H = 0.2 \sim 1.6$ m), the radial distribution of heat transfer coefficient is not uniform. While it remains fairly constant in the central region, the heat transfer coefficient increases dramatically to form a significant peak at a radial position $r/R \approx 0.85 \sim 0.90$, and then decreases towards the wall. This result shows that the solids distribution under DA is fairly uniform in the central region, but solids tend to concentrate near the wall. With the flow developing further down, the peaks in the heat transfer profiles decrease in magnitude and the radial distribution becomes more uniform. More uniform distributions of solids concentration over the bed cross-section are evident in the developed section. Furthermore, the radial profiles of heat transfer coefficient at the same axial location become more uniform with decreasing solids circulation rate under constant superficial gas velocity, because the radial structure of solids concentration becomes more uniform under lower solids circulation rate. The above observation is confirmed by direct measurements of the solids concentration on earlier studies using the same distributor [8].

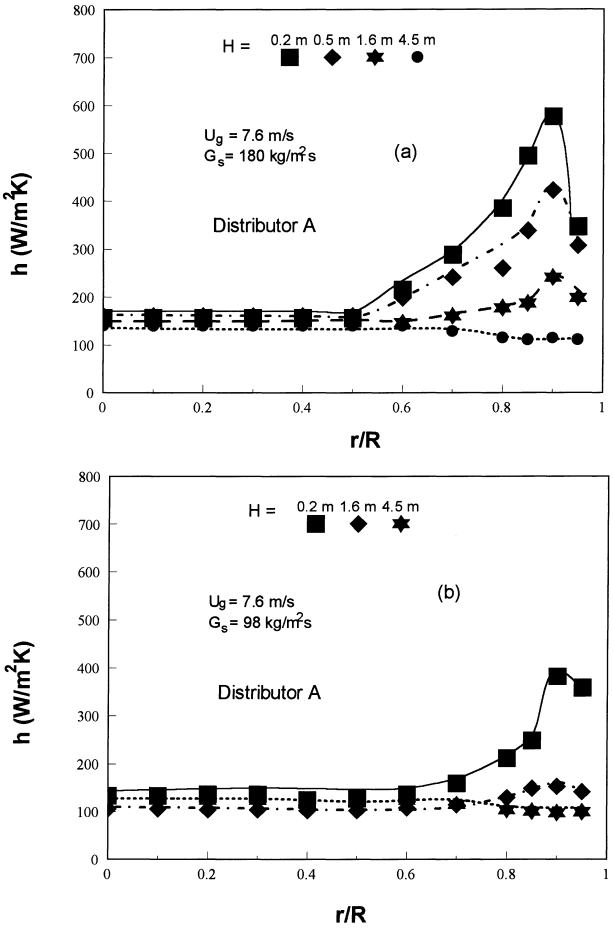

Fig. 5. Radial distributions of heat transfer coefficient with distributor A.

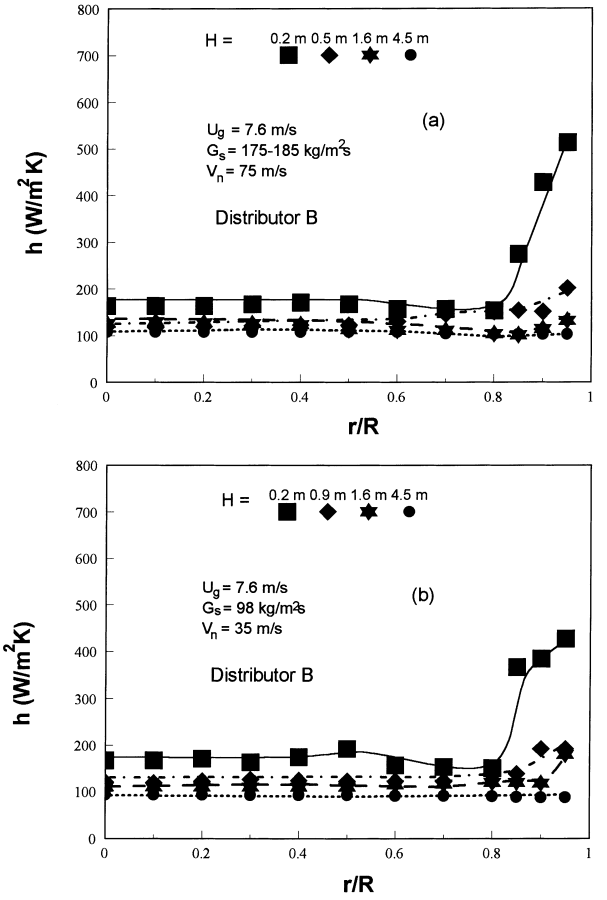

Fig. 6. Radial distributions of heat transfer coefficient with distributor B.

The radial distribution profiles of the heat transfer coefficient measured with distributor B under the same operating conditions with DA are shown in Fig. 6. Comparing the radial heat transfer distribution profiles of DA and DB (Figs. 5 and 6), the effects of the distributors on the radial distributions of heat transfer coefficient is clearly shown. Near distributor B, the radial profiles of the heat transfer coefficient appear to be less uniform as with DA in the central region. Approaching the wall, the radial heat transfer profiles for DB seem not to have a significant peak as evidenced with DA, but increase monotonically toward the wall. This trend is determined by its distributor structure, because DB is made up of seven large diameter feed tubes centered within the column core and away from the wall. The fewer and larger solids distribution tubes could not provide very uniform distribution of solids over the bed cross-section, although the additional high velocity gas jets would help disperse the solids flow as compared to DA [8]. On the other hand, fewer solids are distributed near the wall, so that the heat transfer coefficients there are not as high, and also decrease quickly along the downer. These characteristics all affect the radial distributions of the solids concentration and the heat transfer coefficient in the bed, especially near the distributor.

Under distributor B, it is also found that the heat transfer coefficients increase with the solids circulation rate (Fig. 6), but this effect is not as obvious as compared to distributor A (Fig. 5). Because the nozzle effect help dilute the solids concentration quickly below DB due to rapid solids dispersion and acceleration [8], the effect of solids circulation rate on heat transfer coefficient becomes less significant. It is also found that with DB, the heat transfer coefficients in the central region at the top of the downer (H=0.2 m) are somewhat higher than those with DA because the high velocity gas jets increase the gas convection heat transfer, especially in the center of the bed where solids concentration is lower and gas convection is more important. This outcome not only indicates better solids distribution for DB, but also more enhanced gas–solids mixing [12] immediately below DB, both obvious signs of excellent distributor. Furthermore, it can be seen that the heat transfer coefficient decreases more obviously along the axial direction using DB as compared to DA, suggesting that the gas and solids flow structure development is faster under DB.

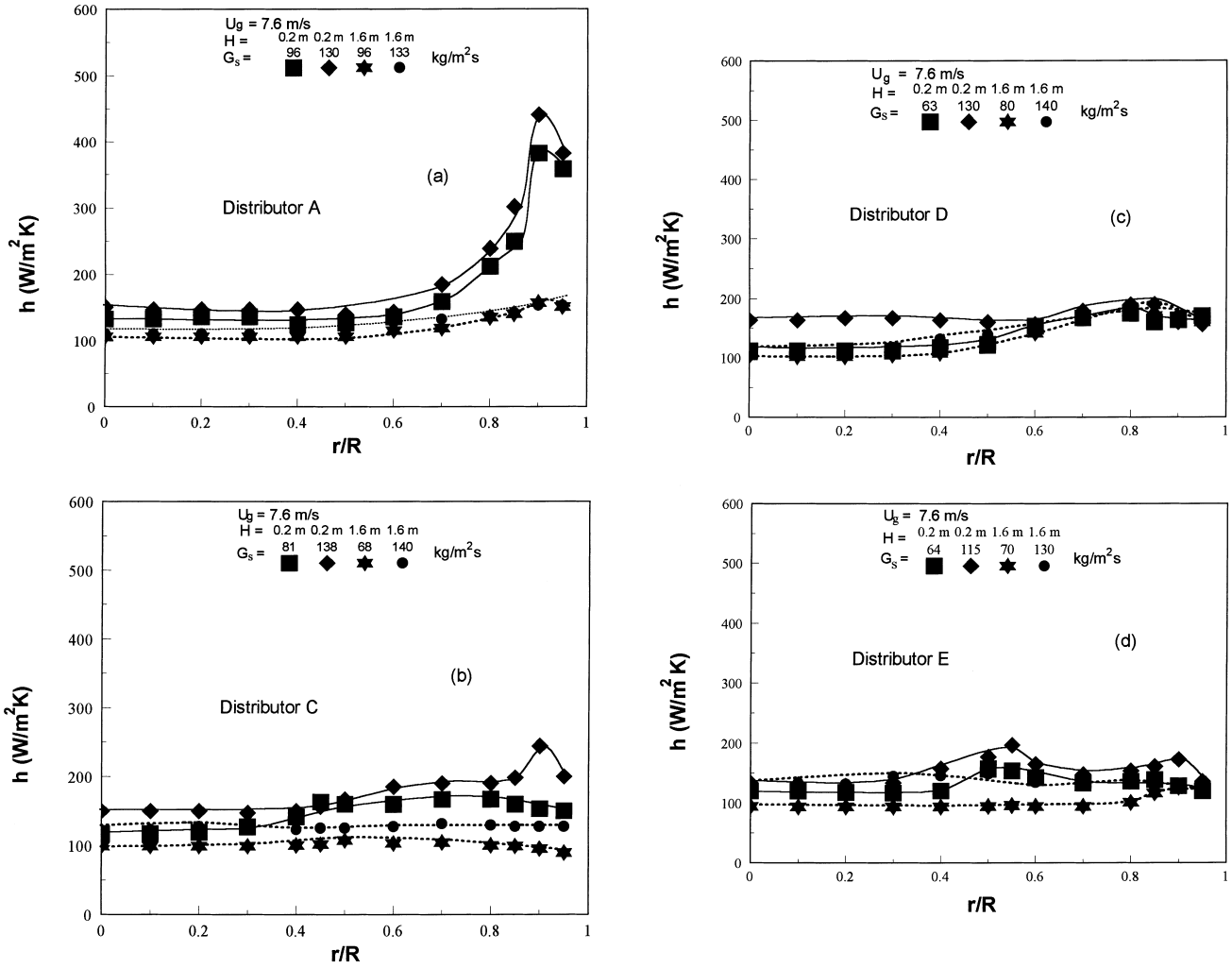

Fig. 7. Radial distributions of heat transfer coefficient with distributors A, C, D and E.

3.3. *The radial distribution of heat transfer coefficient with distributors A, C, D and E*

It is obvious that DA tends to distribute more solids near the wall because of the many solids distribution tubes close to the wall. To investigate the effects of the distributor on the radial solids flow patterns, the heat transfer coefficients were also measured with DC, DD and DE. These distributors have fewer numbers of solids distribution tubes near the wall as compared to DA. The radial distribution profiles of heat transfer coefficient have distinct differences under these distributors, especially immediately below the distributors as shown in Fig. 7. At H=0.2 m, the dramatic peaks that existed at r/R=0.85∼0.90 with DA become less significant with the reduction of solids feed tubes at the wall from DC, DD to DE. The peaks in heat transfer radial distribution profiles are small with DC, less with DD, and finally negligible with DE. This indicates that the radial profiles of solids concentration are sensitive to the distributor structure. With fewer solids distribution tubes near the wall, the radial distributions of solids concentration appear to be more uniform. DA has 18 solids feed tubes located in the annulus which cause the solids concentration to peak near the wall [8], and therefore the heat transfer coefficient profile also peaks in the same radial positions. When the number of plugged solids feed tubes near the wall were increased (DC to DE), the solids congregation near the wall is comparatively prevented, so that the peaks in the radial heat transfer profiles also become gradually insignificant.

Fig. 7 additionally indicates that the radial distribution of the heat transfer coefficient becomes less uniform in the central region when the number of solids distribution tubes is reduced. This is especially true for DE, where half of the solids tubes are blocked. This result may be attributed to the fact that the solids distribution across the downer becomes less uniform when the number of distribution tubes is significantly reduced.

At the axial location of H=1.6 m, the differences in the radial profiles of heat transfer coefficient are indistinguishable. Furthermore the profiles become fairly uniform across the column. This trend suggests that the distributor

effects are only significant in the entrance section of the downer.

3.4. Effect of distributor structure on gas–solid flow development

Summarizing the observations from Figs. 5–7, one can conclude that the distributor design can significantly affect the solids flow development along the downer. Distributor B, with more solids distributed in the core and with the high velocity jets, leads to very rapid flow development and a very uniform radial profile of heat transfer coefficient by a distance of 1.6 m. Distributor E seems to be equally good in promoting uniform solids distribution near the wall and rapid flow development, although it may not be able to provide the intense gas–solids mixing as DB due to the absence of high gas jet. Distributors D and C provide less uniform initial solids distributions and slower flow development, confirming the postulation that a more uniform initial radial solids distribution leads to faster flow structure development. Distributor A with excessive solids distribution near the wall, seems to be a poor downer distributor. On the other hand, all radial profiles of heat transfer coefficients (excluding DA) become fairly uniform by a distance of only 1.6 m from the distributor, indicating that the distributor effects are normally only significant in a very short distance within the downer.

Fig. 8 shows the axial distribution profiles of the average heat transfer coefficients with distributors A and B. It can be seen that with distributor B, the average heat transfer coefficients decrease along the axial direction more rapidly and reach constant valves at higher bed level ($H \approx 2.0$ m) as compared to distributor A, for which this trend seems to be much more gradual. Fig. 8 also shows that the effect of the operating conditions to the axial variations of heat transfer is less significant for DB than for DA. For DB, the high velocity gas jets quickly accelerate the solids so that the effect of the superficial gas velocity and solids circulation rate becomes not very obvious. For DA, however, higher U_g and lower G_s allow rapid solids acceleration, so that the axial profiles stabilize faster under those conditions, but slower otherwise. This confirms again that with distributor B, the gas–solids flow development is faster than with distributor A. This also clearly indicates that the effect of distributors on the gas–solids flow can be well characterized using heat transfer studies.

To analyze the flow development more clearly, the radial nonuniformity index (RNI) proposed by Zhu and Manyele [13] is adapted for the heat transfer coefficient. The resulting radial nonuniformity index, RNI(h), is defined as

$$\mathrm{RNI}(h) = \frac{\sigma(h)}{\sigma(h)_{\max}} = \frac{\sigma(h)}{\sqrt{(h_{\max} - \bar{h})(\bar{h} - h_{\min})}}, \qquad (2)$$

where $\sigma(h)$ is the standard deviation of the radial heat transfer coefficient in the radial direction, $\sigma(h)_{\max}$ is the

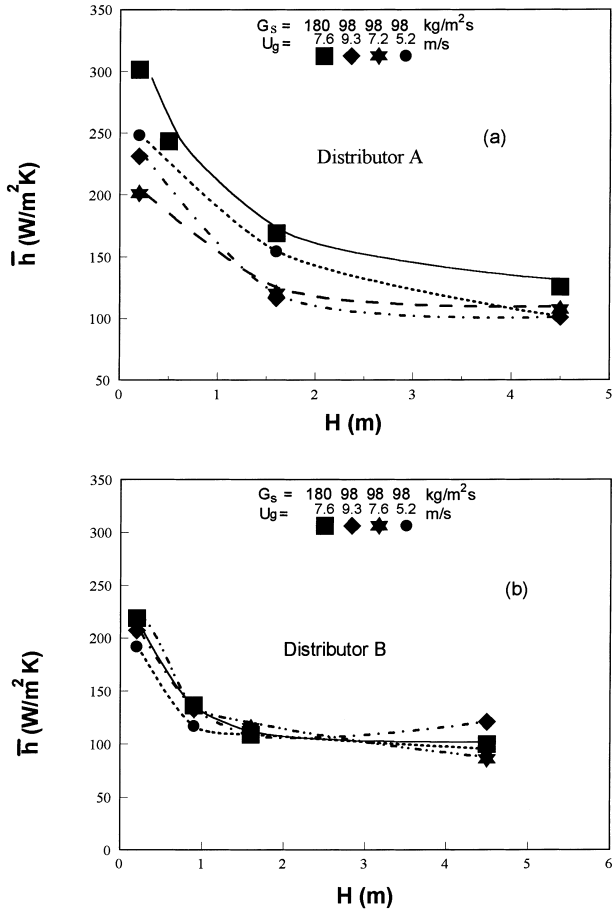

Fig. 8. Axial distributions of the average heat transfer coefficients with distributor A and B.

normalizing parameter which represents the highest possible standard deviation of a series of heat transfer coefficients equaling either $h_{\min}$ or $h_{\max}$, but with the same average as the measured numbers, $h_{\min}$ is the heat transfer coefficient between the gas and the surface in the absence of solids which can be obtained from the equation of forced gas convection [14], $h_{\max}$ is the highest possible heat transfer coefficient which is taken as 600 w/m^{2}K here because the highest heat transfer coefficient measured in this work is approximately 600 W/m^{2}K. This index is bounded by 0 and 1, providing a summary information on the radial distributions of the heat transfer coefficient. A larger number corresponds to a less uniform radial distribution.

Fig. 9 shows a comparison of axial profiles of RNI(h) for distributors A and B. The trend is clear that the RNI decreases down the column and then reaches a constant value. The RNI(h) with DA has higher values near the distributor and decreases more gradually to minimum values. With distributor B, the initial RNI(h) is lower and its decrease with the axial distance is quicker, approaching constant at about 2 m position. This is because in DA, the radial profiles of heat transfer coefficients have large peak

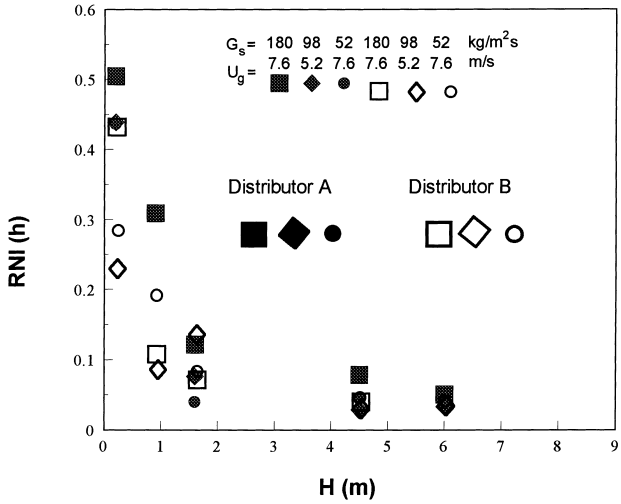

Fig. 9. Axial profiles of RNI(h) for different distributor types.

near the wall and the profiles become uniform more gradually along the downer. For DB, the radial profiles of heat transfer coefficients are more uniform near the distributor and also develop more quickly. These results correspond well to the axial profiles of RNI(ϵ) [8], confirming again that the distributor design has significant effect on the gas and solids flow development as well as the heat transfer behavior in the downer.

4. Conclusion

The effects of distributor design on the gas and solids flow structure in a downer have been studied by measuring the axial and radial distributions of the heat transfer coefficient between the gas–solids flow suspension and a small heat transfer probe using five different types of distributors. This study indicated the following:

1. The heat transfer study can provide a good understanding of the effects of distributors on the gas and solids flow structure and development near the entrance region of the downer.
2. The effect of distributor structure on heat transfer behavior is very significant near the distributor section. The radial distribution profiles of heat transfer coefficient change sensitively with the distributor structure. The variations of the radial distributions of heat transfer coefficient correspond to those of the solids concentration with the same distributor.
3. The gas–solids flow development is different with different distributors. Distributor B, with central solids distribution and high velocity gas jets, provides the best radial distribution. Distributor A, with increased solids distribution near the wall, is shown to give the least uniform initial radial solids distributions. With decreasing number of solids distribution tubes near the wall, distributors C, D and E yield increasingly better distribution.
4. A more uniform initial radial distribution leads to faster flow development in the downer, as seen from the decreased flow development length associated with distributor B, compared to that with distributor A.

5. Nomenclature

A	heat transfer surface area (m^2)
d_p	particle size (μm)
G_s	solids circulation rate (kg/m^{2}s)
h	heat transfer coefficient (W/m^{2}K)
$\bar{h}$	average heat transfer coefficient (W/m^{2}K)
h_{max}	highest possible heat transfer coefficient observed in the downer (W/m^{2}K)
h_{min}	minimum (gas only) heat transfer coefficient in the downer (W/m^{2}K)
H	axial distance from the distributor (m)
I	electric current through the probe (mA)
r/R	reduced radial position
RNI(h)	radial nonuniformity index of heat transfer
RNI(ϵ)	radial nonuniformity index of solids holdup
T_s	surface temperature of the probe (°C)
T_b	average bed temperature (°C)
U_g	superficial gas velocity (m/s)
V	voltage applied on the probe (V)
V_g	gas velocity (m/s)
V_n	nozzle gas velocity (m/s)
V_p	solids velocity (m/s)
ϵ	void fraction
ρ_p	particle density (kg/m^3)
$\sigma(h)$	standard deviation of the radial heat transfer coefficient
$\sigma(h)_{max}$	highest possible standard deviation of heat transfer coefficient

Acknowledgements

The authors are grateful to the Natural Science and Engineering Research Council of Canada for the financial support to the work presented in this paper. Assistance by H. Zhang, P.M. Johnston and J. Ball for the operation of the downer equipment is also gratefully acknowledged.

References

[1] J.R. Grace, A.A. Avidan, T.M. Knowlton (Eds.), Circulating Fluidized Beds, Blackie, London, 1997.
[2] D. Bai, Y. Jin, Z.-Q. Yu, N.-J. Gan, Momentum exchange between gas and solids in a fast fluidized bed, J. Chem. Ind. Eng. (China) 6(2) (1991) 171–181.
[3] F. Wei, J.-X. Zhu, Effect of flow direction on the solids mixing in gas–solids upflow and downflow systems, Chem. Eng. J. 64 (1996) 345–352.

[4] J.-X. Zhu, Z.-Q. Yu, Y. Jin, J.R. Grace, A. Issangya, Cocurrent downflow circulating fluidized bed (Downer) reactors – A state of the art review, Can. J. Chem. Eng. 73 (1995) 662–677.
[5] P.M. Herbert, T.A. Gauthier, C.L. Briens, M.A. Bergougnou, Application of fiber optic reflection probes to the measurement of local particle velocity and concentration in gas–solids flow, Power Technol. 80 (1994) 243–252.
[6] E. Aubert, D. Barreteau, T. Gauthier, R. Pontier, Pressure profiles and slip velocities in a co-current downflow fluidized bed reactor, in: A.A. Avidan (Ed.), Circulating Fluidized Bed Technology IV, AIChE, New York, 1994, pp. 403–405.
[7] F. Wei, J. Liu, Y. Jin, Z. Yu, Hydrodynamics and mixing behaviors in the entrance region of a downer, in: M. Kwauk, J. Li (Eds.), Circulating Fluidized Bed V, Science Press, Beijing, 1996, pp. 122–127.
[8] P.M. Johnston, J.-X. Zhu, H.I. de Lasa, H. Zhang, Effect of distributor design on the initial solids flow development in a downflow circulating fluidized bed, AIChE J. (1998), accepted.
[9] R.L. Wu, C.J. Lim, J.R. Grace, C. Brereton, Instantaneous local heat transfer and hydrodynamics in a circulating fluidized bed, Int. J. Heat Mass Transfer 34 (1991) 2019–2027.
[10] C. Lockhart, J. Zhu, C.M.H. Brereton, C.J. Lim, J.R. Grace, Local heat transfer solids concentration and erosion around membrane tubes in a cold model irculating fluidized bed, Int. J. Heat Mass Transfer 38 (1995) 2403–2410.
[11] H. Zhang, P.M. Johnston, J. Zhu, H.I. de Lasa, M.A. Bergougnou, A Novel calibration procedure for a fiber optic concentration probe, Powder Technol. 100 (1998) 260–272.
[12] Y. Ma, J.-X. Zhu, H. Zhang, Gas–solids contact efficiency in the entrance region of a co-current downflow fluidized bed, Chem. Eng. Res. Des. (1999), in press.
[13] J.-X. Zhu, S.V. Manyele, The use of radial nonuniformity index to characterize radial flow structures in various gas–solids, liquid–solids and three-phase fluidized system, Presented at the 48th Can. Chem. Eng. Conf., October 4–7, 1998, London, Canada.
[14] J.P. Holman, Thermodynamics, 4th ed., McGraw-Hill, New York, 1988.
[15] R.L. Wu, C.J. Lim, J.R. Grace, The measurement of instantaneous local heat transfer coefficients in a circulating fluidized bed, Can. J. Chem. Eng. 67 (1989) 301–307.